

Measurement of the transverse electric field profile of light by a self-referencing method with direct phase determination

C. Bamber,* B. Sutherland, A. Patel, C. Stewart, and J. S. Lundeen

INMS, National Research Council of Canada 1200 Montreal Rd, M-36, Ottawa, K1A 0R6 Canada
*bamberc@nrc.ca

We present a method for measuring the transverse electric field profile of a beam of light which allows for direct phase retrieval. The measured values correspond, within a normalization constant, to the real and imaginary parts of the electric field in a plane normal to the direction of propagation. This technique represents a self-referencing method for probing the wavefront characteristics of light.

©2012 Optical Society of America

OCIS codes: (100.5070) Phase retrieval; (120.2920) Homodyning; (120.3940) Metrology; (120.5050) Phase measurement.

References and Links

1. J. S. Lundeen, B. Sutherland, A. Patel, C. Stewart, and C. Bamber, "Direct measurement of the quantum wavefunction," *Nature* **474**(7350), 188–191 (2011).
2. J. Primot, G. Rousset, and J. C. Fontanella, "Deconvolution from wave-front sensing: a new technique for compensating turbulence-degraded images," *J. Opt. Soc. Am. A* **7**(9), 1598–1608 (1990).
3. R. Q. Fugate, D. L. Fried, G. A. Ameer, B. R. Boeke, S. L. Browne, P. H. Roberts, R. E. Ruane, G. A. Tyler, and L. M. Wopat, "Measurement of atmospheric wavefront distortion using scattered light from a laser guide-star," *Nature* **353**(6340), 144–146 (1991).
4. A. Zhang, C. H. Rao, Y. D. Zhang, and W. H. Jiang, "Novel detecting methods of Shack-Hartmann wavefront sensor at low light levels," *J. Phys.: Conf. Ser.* **48**, 190–195 (2006).
5. G. Sirat and D. Psaltis, "Conoscopic holography," *Opt. Lett.* **10**(1), 4–6 (1985).
6. K. Buse and M. Luennemann, "3D imaging: wave front sensing utilizing a birefringent crystal," *Phys. Rev. Lett.* **85**(16), 3385–3387 (2000).
7. R. W. Gerchberg and W. O. Saxton, "A practical algorithm for the determination of the phase from image and diffraction plane pictures," *Optik (Stuttg.)* **35**, 237–246 (1972).
8. F. Zernike, "How I Discovered Phase Contrast," in *Nobel Lectures, Physics* (Elsevier, 1964), pp. 239–246.
9. S. Fürhapter, A. Jesacher, S. Bernet, and M. Ritsch-Marte, "Spiral interferometry," *Opt. Lett.* **30**(15), 1953–1955 (2005).
10. R. Juanola-Parramon, N. Gonzalez, and G. Molina-Terriza, "Characterization of optical beams with spiral phase interferometry," *Opt. Express* **16**(7), 4471–4478 (2008).
11. G. L. Abbas, V. W. S. Chan, and T. K. Yee, "Local-oscillator excess-noise suppression for homodyne and heterodyne detection," *Opt. Lett.* **8**(8), 419–421 (1983).
12. J. Goodman, *Introduction to Fourier Optics* (Roberts & Co Publishers, 2005).
13. K. A. Nugent, T. E. Gureyev, D. J. Cookson, D. Paganin, and Z. Barnea, "Quantitative phase imaging using hard x rays," *Phys. Rev. Lett.* **77**(14), 2961–2964 (1996).

Introduction

In a recent paper we describe a method for the direct measurement of the quantum wavefunction and, as an experimental example, measure the transverse wavefunction of a single photon [1]. The formalism behind this experiment was developed in the language of quantum physics. This is appropriate because the single-photon nature of light in the experiment only has a quantum optical description. However, since the main components of this experiment make use of conventional optical components, i.e. waveplates, polarizers and photodetectors, and because only intensities rather than correlations are measured, it is not surprising that the classical light analog of the experiment should be describable by conventional electrodynamics. We present this alternative description here. This is not to say

that the general method in Ref [1]. is classical, it will only admit a quantum description in most systems (e.g. if applied to atomic orbitals). Conceptually the classical analog can be viewed as a way of extracting a measurement of the transverse electric field profile (TEFP) of a beam of light by using a self-referencing interferometer.

Various techniques have been developed to measure the TEF of a beam of light. Applications of this type of measurement include a method for adjusting a system with adaptive optics to compensate for atmospheric distortions [2,3], measuring the quality of optical components, surface measurement, and quantifying the quality of optical beams for lithography, holography, and imaging. Some techniques are intended to measure only the phase-front, which is the surface of constant phase of the propagating light beam. One such method is using a Shack-Hartmann sensor, which consists of a lenslet array in front on an imaging detector [4]. This sensor measures the phase gradient at a grid of points which intersect the beam. It has an inherent spatial resolution limitation set by lenslet size. A shear-plate interferometer interferes a shifted copy of the beam with itself, measuring the phase curvature. Similarly, the wavefront from a light wave can also be measured using a technique developed from conoscopic holography where the fields from the ordinary and extraordinary waves are allowed to interfere after passage through a birefringent crystal [5,6]. Another method is the use of the Gerchberg-Saxton algorithm to calculate the phase based on intensity measurements at two planes [7]. This is an iterative fitting technique that can give ambiguous results. Phase-contrast imaging measures small phase shifts imparted by samples [8]. Spiral Interferometry is similar to traditional interferometry but removes phase ambiguities [9,10]. All of the previous techniques are self-referencing in that they do not require a reference beam. A less robust but conceptually simpler technique is that of optical homodyning [11]. In it, measurements of the TEF can be made by mixing the field to be measured with the field of an external reference, a "local oscillator". Unlike the previous techniques, homodyning gives both phase and magnitude of the field directly, without iterative fitting. However this comes at the cost of requiring a phase-stable and well characterized reference local oscillator.

In contrast, we introduce a technique that yields magnitude and phase information directly without requiring an external reference. We experimentally demonstrate that the in-phase and in-quadrature parts of the TEF appear directly as readings on our measurement apparatus to within a normalization constant. Adopting the convention of representing the electric field as a complex-valued quantity, we henceforth refer to these two measurements as the real and imaginary parts of the TEF.

The setup of this experiment is shown in Fig. 1. The experimental approach is to make a series of measurements of the transverse electric field of a beam of polarized light in a plane across the path of the beam. This is accomplished by making a slight rotation of the polarization of the part of the beam that passes through a small half waveplate. Scanning this waveplate transversely allows for a measurement of the complete TEF. Subsequently, the light with zero transverse-momentum is selected. This is done by taking the Fourier transform of the beam with a lens, and filtering the light with a pinhole set at the focus of the lens. The light that passes through the pinhole is subsequently analyzed by measuring the signal imbalance in two detectors receiving the light with polarizations at $\pm 45^\circ$ with respect to the original polarization. This imbalance is proportional to the real part of the transverse electric field at the position of the small $\lambda/2$ waveplate. The imbalance in right/left hand circular polarization is proportional the imaginary part of the transverse electric field at that same waveplate position.

The basis of this measurement is the interference of the light that passes through the sampling halfwave ($\lambda/2$) plate with that portion that goes around it. The pinhole must be made small enough to ensure that the interference occurs at a fixed phase relationship between the probed and unprobed portions of the light. The unprobed light acts as the reference that the probed light interferes with. In this way, the measurement can be described as self-homodyning. The polarization analyzer after the pinhole projects out the real or imaginary

part of the transverse electric field depending on how it is configured. Measuring the intensity difference with a pair of detectors isolates the interference crossterm by canceling out all other contributors.

We have tested this measurement on three TEFP's using a fiber coupled diode laser as our source. The first profile is a truncated Gaussian. To create this profile we use light emerging from a single-mode fiber. This ensures the TEFP is Gaussian, which we then collimated with a lens and truncated by an aperture. The second profile is made narrower by inserting an attenuator with a radial gradient before the collimating lens. The third profile is created by using a window to phase shift half of the beam after the collimating lens.

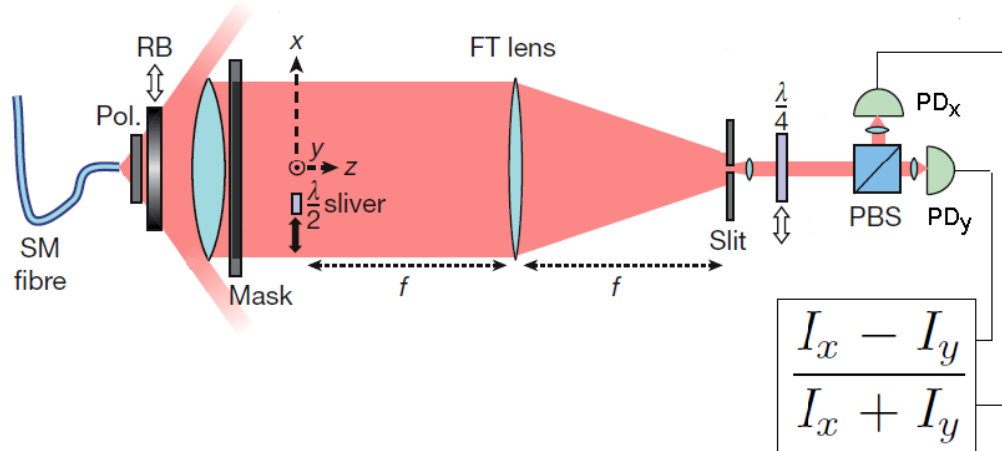


Fig. 1. Experimental setup. The output from a diode laser is injected into a single-mode fibre (SM) and exits at the focus of a collimating lens. The polarization of the beam is set to 45° with a linear polarizer (Pol) immediately after the fibre. A reverse bullseye (apodizing) filter (RB) could be inserted after the polarizer to modify the beam profile. The intention is to measure the real and imaginary parts of the transverse electric field of the beam along the x dimension at the $\lambda/2$ plate ($\lambda/2$ sliver). The lens was masked off with a rectangular aperture that transmitted a narrow strip of light across most of the beamwidth in x. This $\lambda/2$ plate can be scanned across the beam to map out the real and imaginary field profiles. A Fourier Transform (FT) lens takes the Fourier transform of the beam. Only a small portion is transmitted through a slit at the focus. The distance between the half-wave plate and the FT lens is 1m, the focal length of the FT lens (f). Likewise the pinhole is 1m from the FT lens. By measuring the 0° and 90° polarization components of the beam after a polarizing beamsplitter (PBS) with two photodiodes (PD_x & PD_y) and taking the difference over the sum, a measure proportional to the real part of the field is determined. If a quarter-wave ($\lambda/4$) plate is inserted before the PBS, the left-handed and right-handed components of circular polarization can be measured, and the abovementioned ratio is proportional to the imaginary part of the field.

Theory

The electric field associated with a continuous beam of polarized monochromatic light can be written,

$$\vec{E}(\vec{r}, t) = (\varepsilon_x, \varepsilon_y, \varepsilon_z) E_0(x, y, z) \exp(i2\pi\nu t), \quad (1)$$

where $(\varepsilon_x, \varepsilon_y, \varepsilon_z)$ describes the polarization direction, such that $|\varepsilon_x, \varepsilon_y, \varepsilon_z| = 1$. We propose a method to measure the TEFP of a beam in the plane at $z = 0$ defined as

$$TEFP(x, y) = E_0(x, y, 0). \quad (2)$$

Consider a reference frame where the polarization of the beam is oriented at 45° to both the x and y axes. In this case, $\varepsilon_x = \varepsilon_y = \frac{1}{\sqrt{2}}$. A small half-wave plate is introduced to sample

the beam over a small spatial region at $z = 0$ and cause a slight polarization rotation of the portion of the beam that passes through it. The real and imaginary parts of the field may vary over this area, so it is necessary that the $\lambda/2$ plate is small enough that the field is approximately constant over this area. To put it another way, the size of the waveplate is the spatial resolution with which we measure the TEF. By stepping this $\lambda/2$ plate across the beam the overall field profile can be collected. Over the localized region where the polarization has been rotated the polarization vectors are no longer equal. If the polarization is rotated through an angle θ , then the polarization magnitudes in the x- and y- directions become

$$\frac{1}{\sqrt{2}}(\cos \theta + \sin \theta) \text{ and } \frac{1}{\sqrt{2}}(\cos \theta - \sin \theta). \quad (3)$$

After this rotation the transverse electric field x and y polarization components become,

$$E_x(x, y, 0) = \frac{1}{\sqrt{2}} \left((1 - w(x, y)) + w(x, y)(\cos \theta \pm \sin \theta) \right) E_0(x, y, 0), \quad (4)$$

y

where $w(x, y)$ is the rectangular window function, equal to one within the area of the $\lambda/2$ plate, and zero outside. The \pm is to be read + for E_x and - for E_y .

After the beam has been perturbed by the $\lambda/2$ plate, it passes through a lens of focal length f to take the Fourier transform [12]. A pinhole is placed on-axis in the focal plane of the lens. In the plane of the pinhole, $z = z_f$ the field is

$$E_x(x, y, z_f) = \frac{i}{\lambda f} \exp\left(i \frac{2\pi f}{\lambda}\right) \int_{-\infty}^{\infty} \int_{-\infty}^{\infty} \frac{1}{\sqrt{2}} \left((1 - w(x', y')) + w(x', y')(\cos \theta \pm \sin \theta) \right) \times E_0(x', y', 0) \exp\left(-i \frac{2\pi}{\lambda f}(x'x + y'y)\right) dx' dy' . \quad (5)$$

y

The pinhole will only pass the field at $x = y = 0$. This is a good approximation if the field variation is small over the width of the pinhole, i.e.,

$$E_x(0, 0, z_f) = \frac{i}{\lambda f} \exp\left(i \frac{2\pi f}{\lambda}\right) \int_{-\infty}^{\infty} \int_{-\infty}^{\infty} \frac{1}{\sqrt{2}} \left((1 - w(x', y')) + w(x', y')(\cos \theta \pm \sin \theta) \right) \times E_0(x', y', 0) dx' dy' . \quad (6)$$

y

The beam transmitted through the pinhole is collimated, sent through a polarizing beam splitter to separate the x and y polarization components and focused onto photodetectors. The photodetectors measure intensity, which is given by the product of the field with its complex conjugate.

The intensities measured by these two detectors is given by

$$I_x = E_x^*(0, 0, z_f) E_x(0, 0, z_f)$$

y y y

$$= \frac{1}{2(\lambda f)^2} \left[\left| \mathbf{E}_{all\ space} \right|^2 + (\cos \theta - 1 \pm \sin \theta)^2 \left| \mathbf{E}_{waveplate} \right|^2 \right] + (\cos \theta - 1 \pm \sin \theta) \mathbf{Re} \left(\mathbf{E}_{all\ space} \mathbf{E}_{waveplate} \right) \quad (7)$$

where $\mathbf{Re}(a)$ & $\mathbf{Im}(a)$ are the real and imaginary parts of a , and,

$$\begin{aligned} \mathbf{E}_{all\ space} &= \iint_{all\ space} E_0(x', y', 0) dx' dy' \\ \mathbf{E}_{waveplate} &= \iint_{area\ of\ waveplate} E_0(x', y', 0) dx' dy'. \end{aligned}$$

By subtracting the measured intensities at these two detectors and normalizing by the sum of these intensities we get

$$\frac{I_x - I_y}{I_x + I_y} = \frac{2 \sin \theta \left(\mathbf{Re}(\mathbf{E}_{all\ space} \mathbf{E}_{waveplate}) + 2(\cos \theta - 1) |\mathbf{E}_{waveplate}|^2 \right)}{|\mathbf{E}_{all\ space}|^2 + 2(\cos \theta - 1) \mathbf{Re}(\mathbf{E}_{all\ space} \mathbf{E}_{waveplate}) - 2(\cos \theta - 1) |\mathbf{E}_{waveplate}|^2}. \quad (8)$$

This expression has a simplified form in either of two limits. One is the regime where $\mathbf{E}_{all\ space} \gg \mathbf{E}_{waveplate}$, i.e. we need to ensure that the integrated TEF that is probed by the $\lambda/2$ plate, at each position in the $z = 0$ plane, is much smaller than the overall integrated TEF. This can be achieved when the dimensions of the $\lambda/2$ plate are much smaller than the characteristic dimension over which the field is large. The second is the regime where θ is very small. In either case we can make the approximation:

$$\frac{I_x - I_y}{I_x + I_y} \approx \frac{2 \sin \theta \mathbf{Re}(\mathbf{E}_{all\ space} \mathbf{E}_{waveplate})}{|\mathbf{E}_{all\ space}|^2}. \quad (9)$$

Note that the absolute phase of the electric fields is arbitrary and therefore we choose a phase to simplify this expression. In particular, we apply a rotation of $\varphi = \tan^{-1} \left(\frac{\mathbf{Re}(\mathbf{E}_{all\ space})}{\mathbf{Im}(\mathbf{E}_{all\ space})} \right)$ in the complex plane, such that the imaginary part of $\mathbf{E}_{all\ space}$ goes to zero. We rotate all of the beams by this amount to transform to a new coordinate system. In this new coordinate system Eq. (9) becomes

$$\frac{I_x - I_y}{I_x + I_y} \approx \frac{2 \sin \theta \left(\mathbf{Re}(\mathbf{E}_{\varphi waveplate}) \right)}{|\mathbf{E}_{all\ space}|}. \quad (10)$$

We call $\mathbf{Re}(\mathbf{E}_{\varphi waveplate})$ the real part of the TEF, the φ subscript indicating the rotation in the complex plane. It is that part of the transverse electric field which has been probed by the $\lambda/2$ plate that is in phase with the total integrated field.

We next show how the imaginary part of the transverse electric field can be measured. This is the part of the field that is in quadrature with the total integrated field. A quarterwave ($\lambda/4$) plate is inserted between the pinhole and the polarizing beamsplitter with its axis at 45° with respect to the beamsplitter in order to measure the right and left hand polarization components. In contrast to Eq. (6) in this case the two transverse electric field components incident on the detectors are:

$$E_x(0, 0, z_r) = \frac{i}{\lambda f} \exp\left(i \frac{2\pi f}{\lambda} z_r\right) \left((1 \pm i) (\mathbf{E}_{all\ space} + (\cos \theta - 1) \mathbf{E}_{waveplate}) + (1 \mp i) \mathbf{E}_{waveplate} \right) \quad (11)$$

With intensities at the detectors becoming,

$$\begin{aligned}
I_R &= E_R^* (0,0,z_f) E_R (0,0,z_f) \\
&= \frac{1}{(\lambda f)^2} \left[|E_{all\ space}|^2 + ((\cos\theta - 1)^2 + \sin^2\theta) |E_{waveplate}|^2 + 2(\cos\theta - 1) \text{Re}(E_{all\ space} E_{waveplate}) \right. \\
&\quad \left. \pm 2\sin\theta (\text{Re}(E_{all\ space}) \text{Im}(E_{waveplate}) - \text{Im}(E_{all\ space}) \text{Re}(E_{waveplate})) \right] \quad (12)
\end{aligned}$$

It can be shown that if we make the phase rotation as indicated in Eq. (10),

$$\frac{I_R - I_L}{I_R + I_L} \approx \frac{2\sin\theta (\text{Im}(E_{\phi waveplate}))}{|E_{all\ space}|} \quad (13)$$

This measurement projects out the imaginary part of the transverse electric field, $\text{Im}(E_{\phi waveplate})$, that passes through the $\lambda/2$ with the same proportionality constant as the real measurement described earlier. The result is the part of the transverse electric field at the $\lambda/2$ plate that is in quadrature with the total integrated field.

Experiment and results

The source used in this experiment was a continuous-wave diode laser (Sanyo DL7140-201S) operated at a wavelength of 782nm. This laser has a coherence length longer than the thickness of the $\lambda/2$ plate. This ensured that the necessary interference between the sampled beam and the beam that passed around it would occur. The output was coupled into a polarization preserving single mode fiber (Nufern PM780-HP) to ensure a Gaussian spatial mode after launching the beam into free space. The beam was collimated by a 300mm focal length achromatic doublet (Thorlabs AC508-300-B) with a diameter of 50mm after it had passed through a micro-wire polarizer (Edmund Optics NT47-602) which was set to 45° relative to the polarizing beamsplitter located in the analysis part of the setup. The position of the collimating lens was adjusted for best collimation as measured with a shear plate. The beam overfilled this lens such that the Gaussian profile was truncated on the sides.

In principle it is possible to make a two dimensional scan of the transverse electric field of the beam, but for simplicity it was decided to scan in one dimension through the centerline of the beam in the horizontal direction. The beam was masked off with a rectangular aperture 43mm wide in the horizontal direction and 11 mm vertically. The mask was centered on the optic axis of the collimating lens.

The $\lambda/2$ plate used was a true zero order half-wave plate with dimensions 1 mm wide by 25mm high mounted on a 1mm thick supporting glass (BK7) substrate. This optic was centered at the beam height such that the top and bottom were shadowed by the beam mask. This $\lambda/2$ plate was located 65mm downstream from the collimating lens. The birefringent axis was set to provide a 20° rotation of the polarization of the beam passing through it. It was mounted on a horizontal translation stage oriented across the beam with a range such that it could traverse beyond both sides of the mask. This $\lambda/2$ plate was tilted about the x axis such that the optical path difference for 782nm light was an integral number of wavelengths. This was done to eliminate the perturbation of a beam when θ was set to zero. The $\lambda/2$ plate was scanned only in the x direction, through the center of the beam.

The Fourier transform lens was a 1000mm focal length achromatic doublet (Thorlabs AC508-1000-B, diameter 50mm). It was located one focal length downstream of the $\lambda/2$ plate. A 15 micron fixed slit was located at the focus of this lens. This size of slit was sufficient to satisfy the condition that the field variation across it is small, as required in Eq. (6). A slit could be used instead of a pinhole since we were only interested in measuring in one dimension.

We collimated the light emerging from the slit with a 3 cm focal length lens. The light either passed directly or through a $\lambda/4$ plate to a polarizing beamsplitter. At each output port, the photons were focused onto a silicon photodiode (Thorlabs, DET10A). The signal strength

was sufficient that the dominant source of noise was due to fluctuations in the output of the laser. The imbalance in signal between the two detectors is proportional to the real (without the $\lambda/4$ plate) or imaginary (with the $\lambda/4$ plate) part of the probed transverse electric field.

By using a single mode fiber and a well corrected achromat as the source of the beam there was an expectation that the field would have a flat wavefront and that its profile would be a truncated Gaussian. The measurement results are shown in Fig. 2.

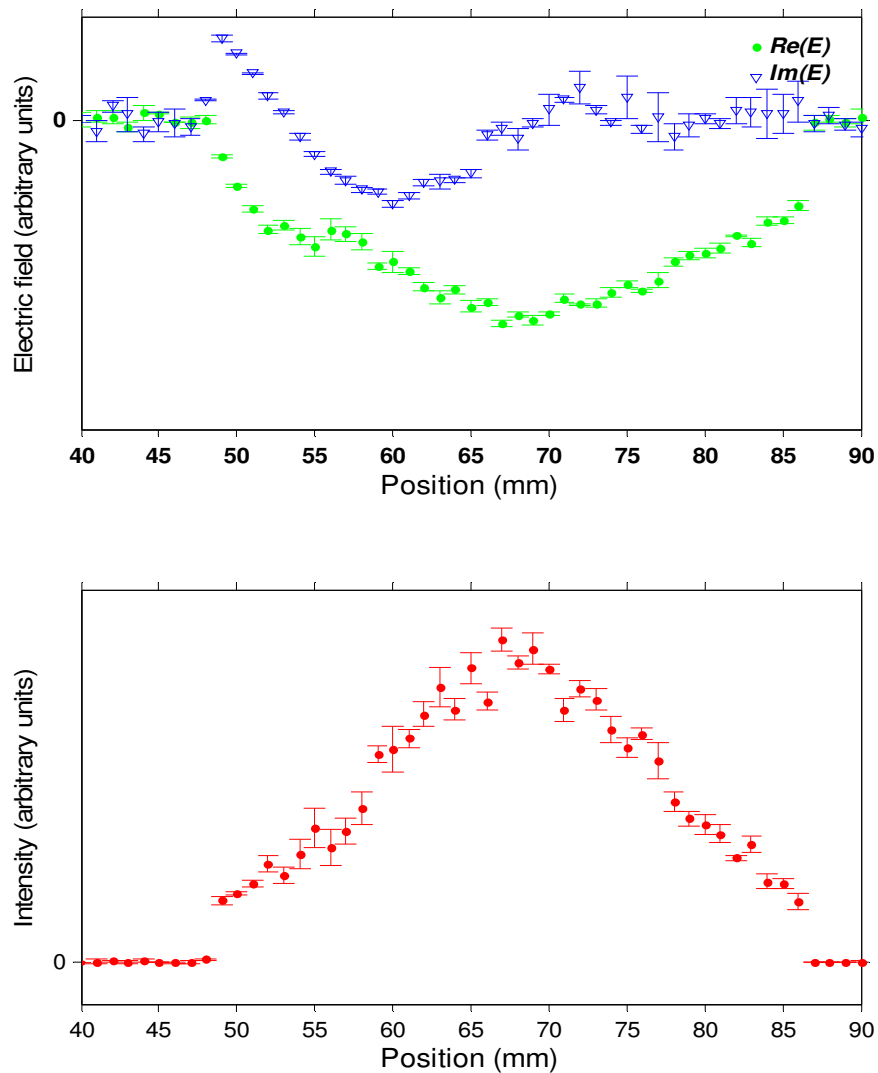


Fig. 2. Real (green dots) and imaginary (blue triangles) measurements of the transverse electric field. The intensity has been calculated as the quadrature sum of the real and imaginary parts. The error bars are statistical and equal to one standard deviation based on the variation in multiple runs.

As can be seen in Fig. 2, the overall profile of the intensity matches the expectation of a truncated Gaussian, but there is a deviation from a flat wavefront as the mix of real and imaginary parts varies transversely. We can calculate the phase as,

$$Phase = \arctan\left(\frac{\text{Re}(E_{\varphi\text{waveplate}})}{\text{Im}(E_{\varphi\text{waveplate}})}\right) \quad (14)$$

This is plotted in Fig. 3.

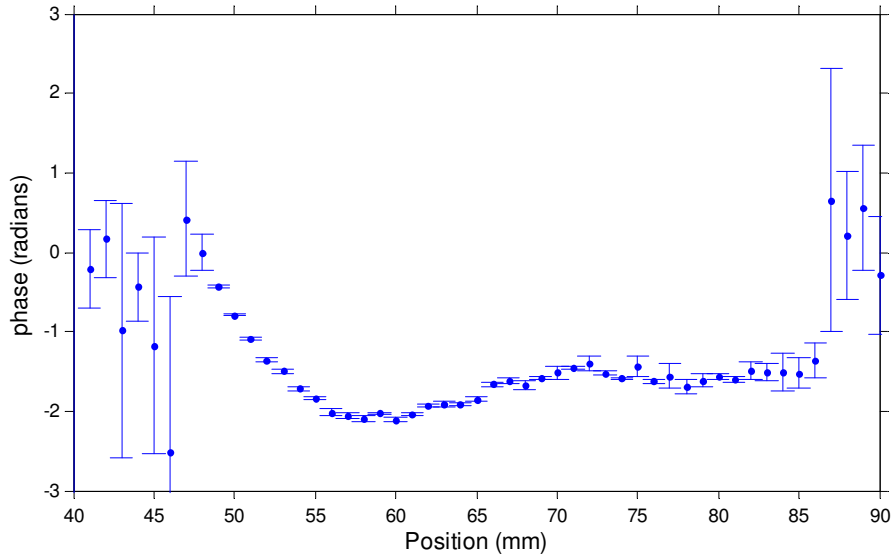


Fig. 3. Phase calculation based on real and imaginary measurements. The error bars are statistical at one standard deviation based on the variation in multiple runs.

Despite our expectation, the phase is not flat.. This could arise from aberrations in the fiber, polarizer or collimating lens or from misalignment of these optics. The lens was measured on a commercial interferometer. The aberrations are of the right magnitude to account for the measured phase but do not agree quantitatively.

We repeat the measurement with a different field profile created by inserting an apodizing filter (EdmundOptics NT64-388) (RB in Fig. 1) into the beam before the 300mm collimating lens, thus reducing the truncation on that lens. The intensity profile was measured by scanning a power meter across the beam. The power meter was masked off to the size of the $\lambda/2$ plate. A comparison of this measurement with the intensity as measured by our technique is shown in Fig. 4. The agreement between these two measurements is a good confirmation of this technique.

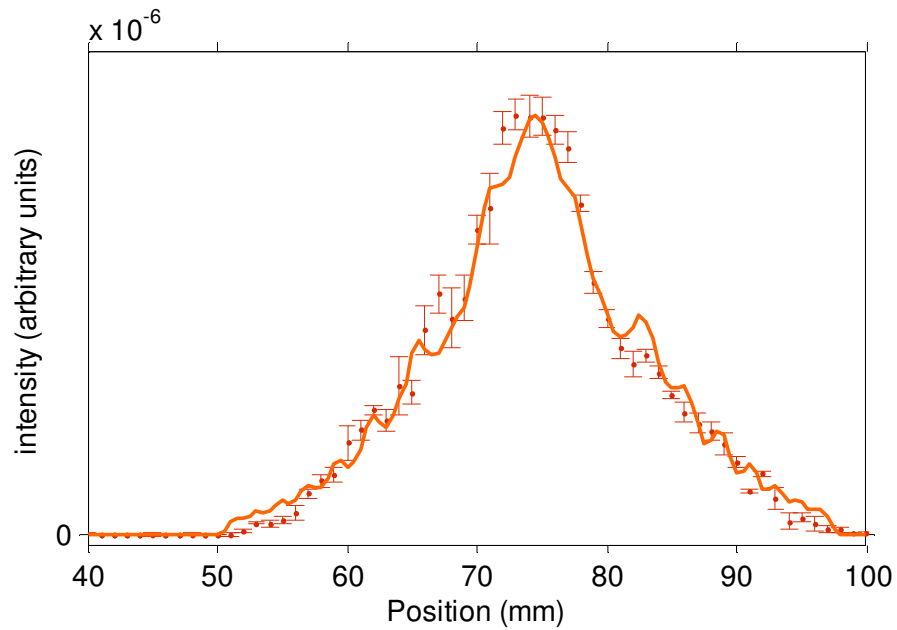


Fig. 4. Measurement with apodizing filter installed to modify beam shape. Comparison of the intensity measured by our technique (data points with error bars) with an intensity measurement made with a power meter (solid line). The error bars are statistical and equal to one standard deviation based on the variation in multiple runs.

We explored a modification to the phase of the beam by placing a glass window of unknown thickness half way across the beam to introduce a phase discontinuity. This data is presented in Fig. 5. In this data we clearly see a discontinuity in the mix of the real and imaginary parts of the field close to the middle of the beam, yet the calculated intensity remains well behaved other than one point directly at the discontinuity. Scattering from the edge of the glass window is responsible for the loss in intensity at this point.

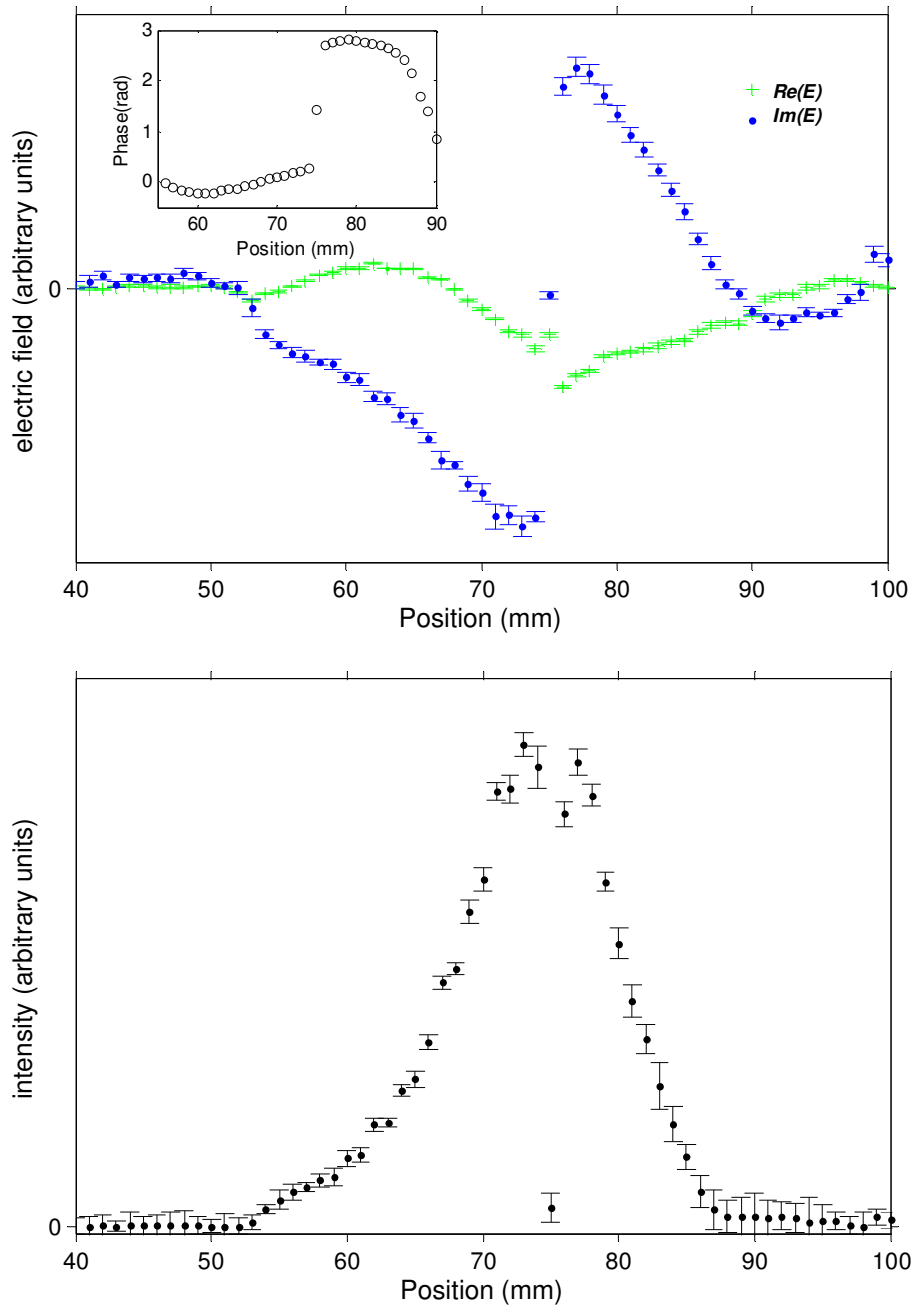


Fig. 5. Real (green dots) and imaginary (blue triangles) measurements of the transverse electric field with a glass plate halfway across the beam. The inset is the phase calculated over the central region of the measurement, showing a clear discontinuity. The intensity is calculated from the measured data.

Conclusions

Experimentally we have demonstrated a direct method of measuring the real and imaginary parts of the transverse electric field associated with a beam of polarized monochromatic light.

Initial measurements show good agreement with prediction. This new technique has some features that differentiate it from other existing techniques. This technique yields the real and imaginary parts of the field directly, without iterative fitting. It is self referencing, in that no external local oscillator is necessary to make a measurement. As a result of this self referencing, it is inherently more stable with respect to phase noise, as the only difference in path between the two interfering fields is the path through the half-wave plate, which is a static optical component. We do not infer the real and imaginary parts of the transverse electric field from the intensity and phase. Each is measured independently and directly. Without relative rescaling we show that they appropriately sum to result in the intensity profile of the beam.

From the measurements of the real and imaginary parts of the transverse electric field the amplitude and phase of the field of propagating beam can be determined. We have found that the statistical errors, at one sigma, on the calculated phase values are of the order of 0.03 radians, or 1/200th of a wave. This technique may have applications in image reconstruction [13] and phase-contrast imaging [8]. One feature of this technique is that the measurement is made in the plane of the leading optic that intercepts the beam, i.e. the $\lambda/2$ plate. This suggests that the technique could be useful for making aberration-free measurements, for example, with space-based telescopes.